

**SYNTHESIS AND CHARACTERIZATION OF
SILICA NANOPARTICLES AND THEIR
APPLICATION AS FILLERS IN
SILICA-BISMALEIMIDE NANOCOMPOSITE**

VEJAYAKUMARAN A/L PADAVETTAN

UNIVERSITI SAINS MALAYSIA

2008

**SYNTHESIS AND CHARACTERIZATION OF
SILICA NANOPARTICLES AND THEIR
APPLICATION AS FILLERS IN
SILICA-BISMALEIMIDE NANOCOMPOSITE**

by

VEJAYAKUMARAN A/L PADAVETTAN

**Thesis submitted in fulfilment of the requirements for the degree of
Doctor of Philosophy**

June 2008

ACKNOWLEDGEMENTS

There are many people that I have to acknowledge and thank for all of their help and support during this research effort. First and foremost, I sincerely acknowledge and am indebted to my main supervisor, Professor Ismail Ab. Rahman for his continued support, motivation, guidance, supervision and help throughout this project.

The second person who deserves my sincere gratitude is my co-supervisor, Dr. Coswald @ Mohd. Nasri for his assistance, encouragement and support in carrying out the polymer related works. Thirdly, I would like to acknowledge Intel Technology (M) Sdn. Bhd. for supplying the financial assistance for this research through generous grants, which also supported my living expenses during the term of my study.

I would like to express my special thanks to the members of Intel Research Group of School of Chemical Sciences, Universiti Sains Malaysia (USM), namely Professor Jamil Ismail, Associate Professor Mohd. Abu Bakar, Dr. Rohana Adnan and Dr. Chee Choong Kooi (Intel) for their advice and guidance throughout my study.

I deeply appreciate the help by Professor M. Bettahar (UHP, France), Professor M. Vergnat (UHP, France) and Associate Professor Farook Adam for their valuable suggestions to analyze and interpret the UV-Vis and Photoluminescence spectra.

I wish to acknowledge all the technical staffs of the School of Chemical Sciences, USM, especially Mr. Aw Yeong, Mr. Yee Chin Leng, Mr. Ong Chin Hin, Mr. Ali Zaini, Mr. Burhanudin, Mr. Kanthasamy and others for their help throughout the course

of this project. I am also grateful to Mr. Pachamuthu, Ms. Jamilah and Mr. Johari from the Electron Microscopy Unit, USM for their tremendous help in conducting the TEM, SEM and EDX analysis. I would like to thank Dr. See Chun Hwa, Ms. Fadzrina, Ms. Wei Wei and others from Intel (M) Sdn. Bhd. for their support and help rendered during the course of DMA and TMA analysis conducted at the Intel facilities in Kulim, Malaysia.

I would also like to thank Universiti Sains Malaysia and School of Chemical Sciences for the facilities and supports provided during my study.

Not forgetting, my sincere appreciations to all my family members especially my fiancée, Ms. Ranjiny Balakrishnan who has been very supportive during my study.

Last but not in the least, I would like to thank my best friends and colleagues, Dr. Ha Sie Tiong, Dr. Yasodha, Dr. Oo Chuan Wei, Dr. Sharon, Mr. Wendy Rusli, Dr. Lim Eng Khoo, Ms. Anis Tasnim, Mrs. Azrat Khan, Mr. Kong Nein Hing, Mr. Ninthia, Ms. Teoh Boon Siew, Ms. Soon Seok Yong, Mr. Chandrasekhar, Mr. Calen Woi, Mr. Yogan, Mr. Vincent Daniel, Mr. Dhevendran, Mr. Ganeson, Mr. Jagatheswaran, Ms. Vanitha, Mr. Mohammad Jafarzadeh, Dr. Sreenivasan and buddies from Sri Ranganatha Swami Madalayam who had helped and encouraged me during my project.

Vejayakumaran Padavettan

June 2008

TABLE OF CONTENTS

	Page
Acknowledgements	ii
Table of contents	iv
List of Tables	x
List of Figures	xiii
List of Abbreviations	xx
Abstrak	xxiii
Abstract	xxvi
CHAPTER ONE – INTRODUCTION	1
1.1 Nanotechnology	1
1.2 Nanoceramics	2
1.2.1 Silica Nanoparticles	2
1.2.1.1 Sol-Gel Process	3
1.2.1.2 Reverse Microemulsion	5
1.2.1.3 Flame Synthesis	6
1.2.2 Applications of Silica Nanoparticles	6
1.2.3 Agglomeration and Aggregation Problems in Silica Nanoparticles	7
1.3 Silica-Polymer Nanocomposites	7
1.3.1 Surface Modification of Silica Nanoparticles	9
1.3.2 Selection of Polymer Matrix	10
1.3.2.1 Epoxies	11
1.3.2.2 Bismaleimide	11
1.4 Problem Statements	12
1.5 Research Objectives	13
1.6 Scope of the Study	14
1.7 Thesis layout	15
References	17
CHAPTER TWO - LITERATURE REVIEWS	22
2.1 Sol-Gel Process	22
2.1.1 Synthesis of Silica Nanoparticles via Stöber Method	26
2.1.1.1 Synthesis of Silica Nanoparticles in the Presence of Electrolytes	26

2.1.1.2	Synthesis of Silica Nanoparticles under Optimized Reaction Conditions	28
2.2	Drying and Agglomeration Phenomena	29
2.3	Size-Dependent Properties of Silica Nanoparticles	31
2.3.1	Physiochemical Properties	31
2.3.2	Thermal and Mechanical Properties	33
2.3.3	Optical Properties	34
2.4	Silica Filled Polymer Nanocomposites	35
2.4.1	Chemical Modification of Silica Surface	37
2.4.2	Methods for Dispersing Silica Nanoparticles in Polymer Matrix	42
2.4.3	Effect of Silica Nanoparticles on the Properties of Nanocomposite	42
2.4.4	Filler-Matrix Interactions	46
2.5	Bismaleimide Polymer Matrix	48
2.5.1	Chemistry of BMI/Diamine	49
2.5.2	Effect of Temperature	51
2.5.3	Reactant Ratios	53
2.5.4	Curing Accelerator	53
2.5.5	Nanocomposites Based on Bismaleimide Polymer Matrix	54
2.6	Characterization Techniques for Nanomaterials	54
	References	59
CHAPTER THREE - MATERIALS AND METHODS		66
3.1	Chemicals	66
3.2	Instruments	67
3.2.1	Sample Preparations and Analytical Conditions	69
3.2.1.1	Transmission Electron Microscope (TEM)	69
3.2.1.2	Scanning Electron Microscope (SEM) and Energy Dispersive X-Ray (EDX)	70
3.2.1.3	Light Microscope (LM)	70
3.2.1.4	Fourier Transformed Infrared (FTIR) Spectroscopy	70
3.2.1.5	Nuclear Magnetic Resonance (NMR) Spectroscopy	71
3.2.1.6	Ultraviolet-Visible (UV-Vis) Spectroscopy	71
3.2.1.7	Photoluminescence (PL) Spectroscopy	71
3.2.1.8	CHN Analysis	71
3.2.1.9	Porosimeter	72
3.2.1.10	Pycnometer	72
3.2.1.11	Differential Scanning Calorimetry (DSC)	73

3.1.1.12	Thermogravimetric Analysis (TGA)	73
3.1.1.13	Dynamic Mechanical Analysis (DMA)	73
3.1.1.14	Thermomechanical Analysis (TMA)	74
3.3	Procedures	75
3.3.1	Synthesis of Silica Nanoparticles (Chapter 4 and 5)	75
3.3.1.1	Effect of Anion Electrolytes on the Particle Size and Morphology	77
3.3.1.2	Effect of Experimental Parameters on the Particle Size and Morphology	79
3.3.2	Effect of Drying Techniques on the Morphology of Silica Nanoparticles (Chapter 6)	79
3.3.2.1	Oven Drying (OD)	80
3.3.2.2	Freeze-Drying (FD)	80
3.3.2.3	Alcohol-Dehydration (AD) Technique	80
3.3.2.4	Characterizations	81
3.3.3	Characterization of Size-Dependent Properties (Chapter 7)	83
3.3.4	Chemical Modifications of Silica Surface (Chapter 8)	83
3.3.4.1	Grafting of Amine Group onto Silica Surface	84
3.3.4.2	Modification of Amine-Modified Silica Surface with BMI monomers	84
3.3.4.3	Grafting of Epoxide Group onto Silica Surface	84
3.3.4.4	Characterization of Surface Modified Silica Nanoparticles	85
3.3.5	Preparation of BMI/DDM Polymer Matrix (Chapter 9)	86
3.3.5.1	Curing Profiles	87
3.3.5.2	Quantitative FTIR Analysis	87
3.3.5.3	Determination of Gel-Time	89
3.3.5.4	Characterization of Thermal Mechanical Properties	89
3.3.6	Preparation of Silica-Bismaleimide Nanocomposite (Chapter 10)	89
3.3.6.1	Labeling of Nanocomposite	90
3.3.6.2	Preparation Methods	90
3.3.6.3	Effect of Silica Nanoparticles on Curing Profile	93
3.3.6.4	Investigating the Filler-Matrix Interactions	93
3.3.6.5	Morphological Examinations	94
3.3.6.6	Characterization of Thermal Mechanical Properties	94
	References	95

CHAPTER FOUR - SYNTHESIS OF SILICA NANOPARTICLES: EFFECT OF ANION ELECTROLYTES ON THE PARTICLE SIZE AND MORPHOLOGY	96
4.1 Introduction	96
4.2 Results and Discussion	98
4.2.1 The Formation of Silica Nanoparticles	98
4.2.2 The Efficiency of Anion Electrolytes in Reducing the Size of Silica Particles	102
4.2.2.1 Conductivity Studies to Understand the Electrolyte Effect	108
4.3 Conclusion	113
References	114
CHAPTER FIVE - SYNTHESIS OF SILICA NANOPARTICLES: AN OPTIMIZED SOL-GEL SYNTHESIS	116
5.1 Introduction	116
5.2 Results and Discussion	117
5.2.1 Effect of TEOS Concentration	117
5.2.2 Effect of R ($[H_2O]/[TEOS]$) Value	121
5.2.3 Effect of Ammonia Feed Rate	124
5.2.4 Effect of Reaction Temperature	126
5.2.5 Ultrasonication versus Magnetic Agitation	129
5.2.6 Synthesis of Silica Nanoparticles under Optimized Conditions	130
5.3 Conclusion	133
References	134
CHAPTER SIX - EFFECT OF DRYING TECHNIQUES ON THE MORPHOLOGY OF SILICA NANOPARTICLES	135
6.1 Introduction	135
6.2 Results and Discussion	136
6.2.1 Efficiency of Various Drying Techniques in Removing Moisture	136
6.2.2 Drying Patterns: LM Studies	139
6.2.3 Morphology of Silica Nanoparticles under Different Drying Conditions: TEM Studies	142
6.2.4 Surface and Pore Analysis	145
6.2.5 Reactions Leading to the Agglomeration of Silica Nanoparticles at Low Temperature	148
6.2.6 Effect of Alcohol-Dehydration Drying Technique on the Morphology of Larger Silica Nanoparticles	149
6.3 Conclusion	154

References	155
CHAPTER SEVEN - CHARACTERIZATION OF SIZE-DEPENDENT PROPERTIES OF SILICA NANOPARTICLES	156
7.1 Introduction	156
7.2 Results and Discussion	157
7.2.1 Variation of Physical Properties with Particle Size	157
7.2.2 Variation of Chemical Properties with Particle Size	161
7.2.3 Variation of Optical Properties with Particle Size	165
7.3 Conclusion	170
References	171
CHAPTER EIGHT - CHEMICAL MODIFICATION OF SILICA SURFACE WITH ORGANO-FUNCTIONAL GROUPS	174
8.1 Introduction	174
8.2 Results and Discussion	175
8.2.1 Optimal Experimental Conditions for Surface Modifications using Silane Coupling Agents	176
8.2.2 Reactions Leading to Modification of Silica Surface: FTIR Analysis	180
8.2.3 Structural Elucidation: NMR Analysis	182
8.2.4 Elemental Analysis of Surface Modified Silica Nanoparticles	190
8.2.5 Reactivity of the Maleimide and Epoxide Groups	192
8.2.6 Thermal Stability of the Surface Modified Silica Nanoparticles	194
8.2.7 Surface Modification of Larger Silica Nanoparticles	198
8.2.8 Effect of Surface Modification on the Size Distributions and Apparent Density of Silica nanoparticles	199
8.3 Conclusion	203
References	204
CHAPTER NINE - PREPARATION OF BISMALIMIDE-DIAMINE POLYMER MATRIX	207
9.1 Introduction	207
9.2 Results and Discussion	208
9.2.1 Effect of BMI/DDM Stoichiometry on the Curing Profiles: DSC Studies	208
9.2.1.1 Effect of DCP on the Curing Profile of BMI/DDM Thermoset	212
9.2.2 Characterization of BMI/DDM Reactions using FTIR Studies	215

9.2.2.1	Effect of DCP on the BMI/DDM Reactions at 150 °C	220
9.2.3	Post-Curing Studies	224
9.2.4	Effect of DCP on the Pot-life	227
9.2.5	Thermal Mechanical Properties of BMI/DDM Thermosets	228
9.2.6	Selection of Optimal BMI/DDM Formulation as the Matrix for Silica-Bismaleimide Nanocomposite	232
9.3	Conclusion	234
	References	235
 CHAPTER TEN - PREPARATION AND CHARACTERIZATION OF SILICA-BISMALEIMIDE NANOCOMPOSITE		237
10.1	Introduction	237
10.2	Results and Discussion	239
10.2.1	Effect of Preparation Conditions on the Filler Dispersion	240
10.2.2	Effect of Fillers on the Curing Profiles of SBN: DSC Studies	243
10.2.3	Characterization of Filler-Matrix Interactions: FTIR Studies	248
10.2.4	Morphological Examinations of the Cured SBN	253
10.2.4.1	Filler Dispersion	253
10.2.4.2	Analysis of Filler Aggregation	257
10.2.5	Thermal Mechanical Properties of SBN	260
10.2.5.1	Viscoelastic Properties	260
10.2.5.2	Thermomechanical Properties	268
10.2.5.3	Thermal Stability	277
10.3	Conclusion	281
	References	283
 CHAPTER ELEVEN - GENERAL CONCLUSION AND RECOMMENDATION FOR FUTURE RESEARCH		289
11.1	General Conclusion	289
11.2	Recommendation for Future Research	293
 APPENDICES		295
LIST OF PUBLICATIONS		318

LIST OF TABLES

	Page	
Table 2.1	Size of the primary particles reported in the literatures	25
Table 2.2	Examples of chemical reactions commonly carried out on ceramics	32
Table 2.3	Silane coupling agents commonly used in the preparation of PMCs	37
Table 2.4	Various types of silica-polymer nanocomposites reported in the literature together with the details on filler sizes, concentrations and some selected results	43
Table 2.5	Examples of the nanocomposites prepared using BMI based matrices	55
Table 2.6	The most common characterization techniques for nanomaterials (<i>NM</i>) and nanocomposites (<i>NC</i>)	56
Table 3.1	Structure of the main chemicals used in this study	67
Table 3.2	List of analytical instruments employed in this study	68
Table 3.3	Conditions used to prepare silica nanoparticles in presence of electrolytes	78
Table 3.4	Variation of experimental parameters used in the second approach to produce silica nanoparticles	79
Table 3.5	Variables used in the preparation of BMI/DDM polymer	86
Table 4.1	Optimal concentrations of each ammonium salts in reducing the size of silica nanoparticles (Particle size of blank sample: 92.3 ± 44.3 nm)	103
Table 4.2	Time (t') that the conductivity starts to become constant for the systems containing various types of anions at its optimal concentrations	111
Table 4.3	Chemical structures of the anions used in this study	111
Table 5.1	Effect of reaction temperature on the silica particle size	128
Table 5.2	The optimized reaction conditions obtained in this study	131
Table 6.1	Water content in the silica samples after various levels of washing in the alcohol-dehydration (AD) technique	137
Table 6.2	Structural and physical properties of the primary silica particles prepared using different drying techniques	138

Table 6.3	Probability of finding the Type 1, Type 2 and Type 3 agglomerates in the silica samples prepared via different drying techniques	143
Table 6.4	Effect of alcohol-dehydration and oven drying techniques on the structural and physical properties of ~ 20 nm and ~ 130 nm silica particles	151
Table 7.1	Summary of the experimental conditions used to produce various sizes of silica nanoparticles via sol-gel process	158
Table 7.2	Effect of particle size on the AS1 band of silica nanoparticles	165
Table 8.1	Characteristic IR absorption of main functional groups present in pure and surface modified S7 samples	182
Table 8.2	Elemental contents of various surface modified 7 nm silica particles (as per grams of silica)	191
Table 8.3	ΔH , T_{onset} and T_{exo} characteristics of Si-GPTS/DDM and Si-APTS-BMI/DDM	194
Table 8.4	Thermal characterization data of pure and surface modified S7 silica samples obtained from TGA-FTIR analysis	196
Table 8.5	Elemental contents of various surface modified S20 and S130 silica particles (as per grams of silica)	198
Table 8.6	The loading (amount) of functional groups on different sizes of silica nanoparticles	199
Table 8.7	Effect of surface modifications on the apparent density of the silica powders	201
Table 9.1	DSC data of pure and admixtures of BMI and DDM prepared at different stoichiometric ratios	210
Table 9.2	DSC data of BMI/DDM prepolymers prepared at 2:1 mol ratio and at different concentrations of DCP	212
Table 9.3	DSC data of BMI/DDM prepolymers prepared at different stoichiometric ratios and containing 0.1 % DCP	214
Table 9.4	Effect of DCP concentration on the extent of polymerization reactions in various BMI/DDM formulations cured at 150 °C for 300 min	224
Table 9.5	Optimal post-curing conditions and the resulting residual maleimide contents in the cured BMI/DDM. The samples were cured at 150°C for 180 min prior to the post-curing process	226
Table 9.6	Gel-time measured at 150 °C for various BMI/DDM/DCP formulations	227
Table 9.7	Thermomechanical properties of BMI/DDM thermosets	229

Table 9.8	Thermogravimetric data measured on BMI/DDM thermosets of different formulations with 0.1 % DCP	232
Table 9.9	Optimal curing conditions and properties of various BMI/DDM thermosets	233
Table 10.1	Details of the silica aggregates observed in the SEM fracture surface of BD-SG7-5 samples at different preparation conditions	242
Table 10.2	DSC data of the exothermic reaction of SBN containing various types of silica nanoparticles at 5.0 and 10.0 wt.%. The concentration of DCP was fixed at 0.1 %	245
Table 10.3	Details of the silica aggregates observed in the SEM fracture surface of SBN containing various types of fillers at 5.0 and 10.0 wt.% filler content	257
Table 10.4	Thermal mechanical properties of neat BMI/DDM and silica-bismaleimide nanocomposites	272
Table 10.5	Thermogravimetric data of pure BMI/DDM (BD) and various types of silica-bismaleimide nanocomposite	280

LIST OF FIGURES

		Page
Figure 1.1	Top-down and bottom-up approaches used to produce nanomaterials	3
Figure 1.2	Flow chart of a typical sol-gel process for preparing nanosilica powder	4
Figure 1.3	Schematic representation of reverse micelles, showing the different regions of a micellar solution: (1) water pool; (2) interface; and (3) organic phase	5
Figure 2.1	Polymerization behavior of aqueous silica	24
Figure 2.2	Electrostatic stabilization of silica nanoparticles in the presence of electrolytes	27
Figure 2.3	Illustration of morphology of dried colloidal silica nanoparticles under: (A) controlled drying and (B) drying in presence of water and catalyst that leads to wet-ageing process, resulting in agglomeration phenomena	30
Figure 2.4	Measured and calculated specific surface areas of silica spheres of different size. A rigid sphere with smooth surface is assumed in the calculation	33
Figure 2.5	Normalized PL spectra of different sizes of silica nanoparticles as reported by Chen	35
Figure 2.6	Qualitative illustration of surface modification of silica surface using silane coupling agent via (a) non-aqueous and (b) aqueous route	39
Figure 2.7	Possible reaction mechanism between amine modified silica surface and NPM as proposed by Shen et al.	41
Figure 2.8	(a) complex modulus and damping, and (b) first and second glass transition temperatures (T_g and T_β) as a function of nanosilica volume fraction, as reported by Zhang et al.	45
Figure 2.9	SEM micrographs of fractured epoxy nanocomposites filled with (a) pure silica and (b) surface modified (with epoxide functionalities) silica nanoparticles by 70 wt.% as reported by Kang et al.	47
Figure 2.10	The general structure of BMI	48
Figure 2.11	Chemical reactions that occur during the polymerization of a BMI with an amine: chain extension (I), secondary amine cross linking (II) and BMI homopolymerization (III)	50

Figure 2.12	DMA spectra of BMI prepared at different post-curing temperatures. L-BMI: 218 °C and H-BMI: 230 °C	52
Figure 3.1	Schematic illustration of the relationship between storage modulus (E') and temperature for a typical BMI polymer. The glass transition temperature, T_g was determined by intercept method as shown by the dashed lines	74
Figure 3.2	Schematic illustration of the relationship between dimensional change and temperature of a thermosetting polymer. The glass transition temperature, T_g was determined from the onset deflection point as shown by the dashed lines. The CTE was determined from the slope of the curve, before and after the T_g	75
Figure 3.3	Standard method used to synthesize silica nanoparticles: (a) investigating the effect of electrolytes and (b) investigating the reaction parameters that affect the particle size (optimization of reaction parameters)	77
Figure 3.4	Standard method used to produce the BMI/DDM thermosetting polymer	87
Figure 3.5	Procedures used to disperse silica nanoparticles in MI	92
Figure 3.6	Procedures used to disperse silica nanoparticles in MII	92
Figure 3.7	Procedures used to disperse silica nanoparticles in MIII	93
Figure 4.1	Effect of ammonia concentration on particle size and yield of silica particles prepared at other fixed conditions	99
Figure 4.2	Effect of ammonia concentration on particle size distribution of silica	100
Figure 4.3	TEM micrographs of silica nanoparticles synthesized at different concentration of ammonia; (a) 0.78, (b) 1.23, (c) 1.87, (d) 3.29 and (e) 5.27 mol/L at other fixed conditions	101
Figure 4.4	Particle size versus concentration of different ammonium salts	103
Figure 4.5	Particle size distribution of silica prepared at different concentration of (a) NH_4Cl , (b) NH_4Br , (c) NH_4I , (d) NH_4NO_3 and (e) $(\text{NH}_4)_2\text{SO}_4$	104
Figure 4.6	TEM micrographs of silica nanoparticles synthesized in the presence of ammonium salts; (a) NH_4Cl 10^{-5} mol/L, (b) NH_4Br 10^{-6} mol/L, (c) NH_4I 10^{-6} mol/L, (d) NH_4NO_3 10^{-4} mol/L and (e) $(\text{NH}_4)_2\text{SO}_4$ 10^{-5} mol/L at other fixed conditions	106
Figure 4.7	FTIR spectra of silica nanoparticles synthesized in presence of NH_4Br at 10^{-6} mol/L, (a) before and (b) after calcination	107
Figure 4.8	Ionic conductivity vs ionic radius of anions present in the reaction medium at the concentration of 10^{-6} mol/L	109

Figure 4.9	Ionic conductivity of the reaction medium containing different concentrations of Br ⁻ ion as a function of time compared to blank sample	110
Figure 5.1	Effect of TEOS concentration on particle size and yield of silica nanoparticles prepared at other fixed conditions	118
Figure 5.2	Effect of TEOS concentration on particle size distributions of silica	119
Figure 5.3	TEM micrographs of silica nanoparticles synthesized at different concentration of TEOS; (a) 0.13, (b) 0.25, (c) 0.70, (d) 1.03 and (e) 1.65 mol/L, at other fixed conditions	120
Figure 5.4	Effect of R values on particle size and yield of silica nanoparticles prepared at other fixed conditions	121
Figure 5.5	Effect of R values on particle size distributions of silica	122
Figure 5.6	TEM micrographs of silica nanoparticles synthesized at different R values; (a) 1.3 (b) 9.3, (c) 18.5, (d) 37.0 and (e) 55.6, at other fixed conditions	123
Figure 5.7	Effect of NH ₃ feed rate on particle size and yield of silica nanoparticles synthesized at other fixed conditions	124
Figure 5.8	Effect of NH ₃ feed rate on particle size distributions of silica	125
Figure 5.9	Effect of NH ₃ feed rate on pH profile of the sol-gel system	126
Figure 5.10	TEM micrographs of silica nanoparticles synthesized at different NH ₃ feed rate; (a) 0.40, (b) 0.20, (c) 0.10, (d) 0.05 and (e) 0.03 mL/min, at other fixed conditions and (f) micrograph of commercial fumed silica particles ($d = 17.1 \pm 5.9$ nm)	127
Figure 5.11	Effect of reaction temperature on particle size distribution of silica	128
Figure 5.12	TEM micrographs of the silica nanoparticles prepared at (a) 45 °C and (b) 65 °C, at other fixed conditions as given in Table 3.3 of Chapter 3	129
Figure 5.13	TEM micrographs of the silica particles prepared at fixed conditions under the influence of (a) MA and (b) US	130
Figure 5.14	TEM micrographs of ultrafine silica nanoparticles prepared at optimal experimental conditions at the magnification of (a) 55k and (b) 340k	131
Figure 5.15	Particle size distributions of ultrafine silica nanoparticles prepared at optimal experimental conditions	132
Figure 6.1	FTIR spectra of the supernatants (liquid) collected after first and fifth agitation of primary silica using alcohol-dehydration technique as compared to the spectra of pure TEOS and EtOH	139

Figure 6.2	Drying patterns of the freshly synthesized primary silica observed under optical microscope after (a) OD, (b) FD, (c) AD and (d) typical drying pattern of the suspension containing processed powder. Scale bar 100 μm	140
Figure 6.3	Particle size distribution of the primary silica particles prepared via different drying techniques	143
Figure 6.4	Types of agglomerates found in the samples prepared via different drying techniques. The average size of agglomerate, D_{ag} given in the brackets were calculated based on: $D_{\text{ag}} = (D_L + D_S)/2$, where D_L and D_S is the longest and shortest length of the agglomerate	144
Figure 6.5	(a) Nitrogen adsorption-desorption isotherms and (b) pore size distribution for primary silica particles prepared using different drying techniques: (1) AD, (2) FD and (3) OD	147
Figure 6.6	Particle size distribution of S20 and S130 silica samples prepared via different drying techniques	150
Figure 6.7	TEM micrographs of processed (a) S20 and (b) S130 silica particles, prepared via OD and AD techniques	153
Figure 7.1	Size distribution of various sizes of silica nanoparticles used in this study	158
Figure 7.2	Variation of apparent density (D_a) with particle size (analysis error: 0.7 – 2.8 %)	159
Figure 7.3	Variation of BET specific surface area with particle size (analysis error: 0.5 – 1.6 %)	161
Figure 7.4	Variation of silanol concentration (δ_{OH}) and silanol number (α_{OH}) with particle size (analysis error: 2.9 – 4.8 %)	162
Figure 7.5	FTIR spectra of various sizes of silica nanoparticles. The insert shows the magnification of the peaks corresponding to Si-O-Si stretching vibrations	164
Figure 7.6	Optical absorption spectra of various sizes of silica nanoparticles	167
Figure 7.7	Lambda max (λ_{max}) of the UV-Vis spectra as a function of particle size (analysis error: 4.8 – 6.3 %)	167
Figure 7.8	Photoluminescence (PL) spectra of various sizes of silica nanoparticles	168
Figure 8.1	Proposed reaction scheme between APTS and silanol groups of silica surface based on flip mechanism	177
Figure 8.2	Proposed reaction scheme between GPTS and silanol groups of silica surface	178

Figure 8.3	The variation of carbon/nitrogen loading with the volume of (a) APTS and (b) GPTS as determined from the elemental analysis	179
Figure 8.4	FTIR spectra of pure and various surface modified S7 samples	181
Figure 8.5	Proposed reaction scheme between primary amine and maleimide double bonds describing the nucleophilic addition mechanism	183
Figure 8.6	²⁹ Si CP/MAS NMR spectra of pure and various surface modified S7 silica samples	184
Figure 8.7	¹³ C CP/MAS NMR spectra of pure silica and pure BMI together with the BMI structure	186
Figure 8.8	¹³ C CP/MAS NMR spectra of Si-APTS together with the proposed structure	187
Figure 8.9	¹³ C CP/MAS NMR spectra of Si-APTS-BMI together with the proposed structure	189
Figure 8.10	¹³ C CP/MAS NMR spectra of Si-GPTS together with the proposed structure	190
Figure 8.11	The proposed reaction mechanism between DDM and (a) Si-GPTS and (b) Si-APTS-BMI	192
Figure 8.12	DSC graphs of pure and various surface modified 7 nm silica particles mixed with DDM (1:1 wt. ratio)	193
Figure 8.13	Weight loss curve (TG) and first derivative of weight loss curve (DTG) of (a) pure silica (S7), (b) Si-APTS, (c) Si-APTS-BMI and (d) Si-GPTS obtained through TGA analysis	195
Figure 8.14	Effect of surface modifications on the particle size distribution of (a) ~ 7 nm, (b) ~ 20 nm and (c) ~ 130 nm silica particles	200
Figure 9.1	DSC thermograms of pure and admixtures of BMI and DDM at different stoichiometric ratios	209
Figure 9.2	Proposed reaction mechanisms for various reactions occurring in BMI/DDM polymer system	211
Figure 9.3	FTIR spectra of 2:1 (BMI/DDM) prepolymer cured at 150 °C as a function of curing time, in the range of (a) 4000 – 1435 cm ⁻¹ and (b) 1595 – 855 cm ⁻¹	216
Figure 9.4	Concentration of various functional groups as a function of time for (a) 2:1, (b) 3:1 and (c) 4:1 BMI/DDM formulations cured at 150 °C	218
Figure 9.5	Concentration of various functional groups as a function of time for (a) 2:1, (b) 3:1 and (c) 4:1 BMI/DDM formulations at 0.1 % of DCP, cured at 150 °C	221

Figure 9.6	Effect of post-curing on the total conversion of maleimide double bonds for the 2:1 BMI/DDM formulation in presence and absence of 0.1 % DCP	225
Figure 9.7	Temperature dependence of the storage modulus (solid line) and $\tan \delta$ (dashed line) of the cured BMI/DDM thermosets (a) in presence and (b) absence of 0.1 % DCP	231
Figure 10.1	SEM-EDX Si mapping microscopic micrographs of BD-SG7-5 prepared via (a) MI , (b) MII and (c) MIII . Images at left were taken at 500x while at the right were taken at 10000x	241
Figure 10.2	Size distribution of silica aggregates found in the SEM fracture surface of SBN containing SG7 at 5.0 wt.% filler content, prepared via different preparation conditions	242
Figure 10.3	DSC thermograms of BMI/DDM/SiO ₂ admixtures containing various surface modified 7 nm silica particles at 5.0 wt.% filler content with 0.1 % DCP	244
Figure 10.4	Normalized FTIR spectra of pure silica and cured BD (BMI/DDM) polymer matrix as compared to the cured SBN containing 5.0 and 10.0 wt. % of S7	249
Figure 10.5	Normalized FTIR spectra of SG7 and cured BD (BMI/DDM) polymer matrix as compared to the cured SBN containing 5.0 and 10.0 wt. % of SG7	251
Figure 10.6	Normalized FTIR spectra of SB7 and cured BD (BMI/DDM) polymer matrix as compared to the cured SBN containing 5.0 and 10.0 wt. % of SB7	251
Figure 10.7	Normalized FTIR spectra of cured SBN containing various sizes of silica nanoparticles modified with epoxide pendant groups at 10.0 wt.% filler content	252
Figure 10.8	SEM micrographs (left) and the corresponding EDX mapping of Si elements (right) of fractured SBN filled with (a) S7, (b) SB7 and (c) SG7 by 5.0 wt.% filler content. Magnification = 500x	254
Figure 10.9	SEM micrographs (left) and the corresponding EDX mapping of Si elements (right) of fractured SBN filled with 10.0 wt.% SG7 at (a) 500x and (b) 10000x magnifications	255
Figure 10.10	High magnification SEM micrographs of SBN containing SG7 at (a) 5.0 and (b) 10.0 wt.% filler content	256
Figure 10.11	High magnification SEM micrographs showing the silica aggregates observed in (a) BD-S7-10 and (b) BD-SG7-10 samples	259
Figure 10.12	Temperature dependence of storage modulus (solid line) and $\tan \delta$ (dashed line) of silica-bismaleimide nanocomposite containing (a) S7, (b) SB7 and (c) SG7 at various concentrations	261

Figure 10.13	Storage modulus as a function of silica concentration for the nanocomposites filled with (a) various surface modified 7 nm particles and (b) different sizes of particles modified with epoxide groups	263
Figure 10.14	Temperature dependence of storage modulus (solid line) and $\tan \delta$ (dashed line) of silica-bismaleimide nanocomposite containing different sizes of silica particles modified with epoxide groups at 5.0 wt.% filler content	267
Figure 10.15	Variation of dimensional change with the temperature for pure BMI/DDM (BD) and nanocomposites filled with various surface modified silica nanoparticles at 5.0 wt.% filler content	268
Figure 10.16	Variation of CTE below T_g (α_1) with the filler concentration for (a) various types of 7 nm silica particles and (b) various sizes of silica nanoparticles modified with epoxide groups	270
Figure 10.17	Variation of T_g (from TMA) with the filler concentration for (a) various types of 7 nm silica particles and (b) various sizes of silica nanoparticles modified with epoxide groups	274
Figure 10.18	TEM micrographs of (a) SG20 and (b) SG130. Diameter of the individual particles: SG20: 21.3 nm; SG130: 136.4 nm	276
Figure 10.19	TGA thermograms for the SBN filled with (a) S7, (b) SB7 and SG7 at various filler contents	278

LIST OF SYMBOLS, ABBREVIATIONS AND NOMENCLATURE

(Sample notations or abbreviations are given in Chapter 3)

Symbols	Descriptions
[MI]	Concentration of maleimide double bonds
[MI] _{homopolym}	[MI] consumed for homopolymerization cross-linking reaction
[PA]	Concentration of primary amine
[SA]	Concentration of secondary amine
[TA]	Concentration of tertiary amine
AD	Alcohol dehydration
α_{OH}	Silanol number
APTS	3-aminopropyltrimethoxysilane
AS1	Si-O-Si asymmetrical stretching
BMI	Bismaleimide or 1,1'-(Methylenedi-4,1-phenylene)bismaleimide
BMI/DDM or BD	Bismaleimide/4, 4'-diaminodiphenylmethane
CTE	Coefficient of thermal expansion
α_1	CTE below T_g
α_2	CTE above T_g
CVC	Chemical vapor condensation
d	Average diameter of particles
δ	Bending vibration
D_a	Apparent density
DABPA	O',O-diallyl bisphenol A
DCM	Dichloromethane
DCP	Dicumylperoxide
DDM	4, 4'-diaminodiphenylmethane
ΔH	Enthalpy
DLMCA	Diffusion limited monomer-cluster aggregation
DMA	Dynamic mechanical analysis
δ_{OH}	Silanol concentration
D_p	Pore size
D_t	True density
ε	Paramagnetic defect sites

Symbols	Descriptions
E'	Storage modulus
EDL	Electrical double layer
EDX	Energy dispersive X-ray
eV	Electron volt
FD	Freeze drying
FTIR	Fourier transform infrared
GPTS	3-glycidyloxypropyltrimethoxysilane
K	Ionic conductivity measured in μS (micro Siemens)
t'	Time where K become constant
LM	Light microscope
λ_{max}	Lambda maximum
MA	Magnetic agitation
MCA	Monomer-cluster aggregation
ν	Stretching vibration
N_A	Avogadro number (6.022×10^{23})
ν_{as}	Asymmetric stretching vibration
NH_4X	Ammonium salts
NMR	Nuclear magnetic resonance
NPM	<i>N</i> -phenyl maleimide
OD	Oven drying
ODC	Oxygen deficient centers
P	Probability of finding agglomerates in silica powder
PAAM	Polyacrylamide
phr	Part per hundred resin
PL	Photoluminescence
PMC	Polymer matrix composite
PSD	Particle size distributions
θ	Si-O-Si bond angle
QBSD	Backscattering mode
R	$[\text{H}_2\text{O}]/[\text{TEOS}]$ ratio
<i>R'</i>	Organo-functional groups
RLMCA	Reaction limited monomer-cluster aggregation
RM	Reverse microemulsion

Symbols	Descriptions
R_s	$SSA_{BET}/SSA_{Theoretical}$
σ	Standard deviation of particle size
SAXS	Small angle X-ray scattering
SBN	Silica-Bismaleimide Nanocomposite
SE	Secondary electron mode
SEM	Scanning electron microscopy
$Si(OR)_3R'$	Silane coupling agent
SSA	Specific surface area
SSA_{BET}	BET specific surface area
$SSA_{Theoretical}$	Theoretical specific surface area
STE	Self-trapped exciton
T	Temperature ($^{\circ}C$)
$\tan \delta$	Damping behavior
T_d	Decomposition temperature
TEM	Transmission electron microscopy
TEOS	Tetraethylorthosilicate
T_g	Glass transition temperature
T_{β}	Beta transition temperature
TGA	Thermogravimetric analysis
TMA	Thermomechanical analysis
US	Ultrasonic
UV-Vis	Ultraviolet-visible
V_{mp}	Micropore volume
V_p	Pore volume

SINTESIS DAN PENCIRIAN SILIKA NANOZARAH DAN PENGGUNAANYA SEBAGAI PENGISI DI DALAM NANOKOMPOSIT SILIKA-BISMALEIMIDA

ABSTRAK

Penyelidikan yang dijalankan adalah untuk mengkaji pembentukan, pertumbuhan dan kaedah pengawalan saiz zarah silika melalui proses sol-gel dengan menggunakan tetraetoksilikat (TEOS) sebagai pemula dalam keadaan bes. Pembentukan dan pertumbuhan zarah silika didapati sangat dipengaruhi oleh kepekatan NH_3 (mangkin). Sol yang stabil telah terbentuk pada kepekatan NH_3 yang rendah manakala kepekatan yang tinggi telah menghasilkan zarah yang besar dan berbentuk sfera dengan saiz dalam julat 90 – 700 nm. Pendekatan pertama secara penambahan sedikit garam ammonium (NH_4X) telah menghasilkan silika nanozarah yang tersebar dengan saiz 20.5 hingga 34.1 nm. Ini bergantung kepada saiz dan kepekatan anion yang hadir di dalam sistem. Pendekatan kedua telah digunakan untuk mengurangkan lagi saiz zarah silika melalui pengoptimuman parameter tindak balas seperti kepekatan TEOS, nilai R (nisbah kepekatan air terhadap TEOS), kadar penambahan NH_3 dan suhu tindak balas. Zarah silika yang sangat halus dan tersebar dengan saiz 7.1 ± 1.9 nm yang berada di dalam julat zarah asas telah berjaya dihasilkan pada keadaan optimum. Silika nanozarah yang dihasilkan kemudiannya disebar dan dikeringkan dengan menggunakan kaedah penyahidratan-alkohol (AD). Kaedah ini merupakan suatu kaedah pengeringan yang baru, mudah dan rendah kosnya serta mampu mengurangkan penggumpalan dan meningkatkan sebaran silika nanozarah berbanding kaedah pengeringan beku (FD) and pengeringan ketuhar (OD). Silika nanozarah yang telah diproses mempunyai beberapa sifat menarik yang bergantung kepada saiz. Peningkatan luas permukaan spesifik (SSA) and kepekatan silanol (δ_{OH}) yang nyata serta peningkatan ketumpatan ketara (D_a) yang

beransur telah diperhatikan apabila saiz zarah dikurangkan daripada 400 kepada 7 nm. Selain itu, pengurangan nombor silanol (α_{OH}) dan sudut ikatan Si-O-Si serta kewujudan kecacatan aktif-optik pada saiz zarah yang lebih kecil mencadangkan bahawa perubahan ketara berlaku pada struktur nanosilika. Pengubahsuaian permukaan silika secara kimia telah dijalankan dengan mencantum kumpulan epoksida and maleimida. Kumpulan epoksida telah dicantum dengan menggunakan 3-glisidiloksi-propiltrimetoksisilana (GPTS) manakala kumpulan maleimida telah dicantum melalui tindak balas 1,1'-(Metilenadi-4,1-fenilena)bismaleimida (BMI) kepada silika nanozarah yang terlebih dahulu dicantumkan dengan kumpulan amina menggunakan 3-aminopropiltrimetoksisilana (APTS). Kedua-dua kumpulan epoksida dan maleimida yang didapati terikat secara kovalen pada permukaan silika adalah reaktif. Muatan kumpulan berfungsi didapati meningkat dengan pengurangan saiz zarah, sebagai contoh 130 nm (1.09 mmol/g) < 20 nm (1.70 mmol/g) < 7 nm (2.04 mmol/g) bagi kumpulan epoksida. Matriks untuk nanokomposit silika-bismaleimida (SBN) telah disediakan daripada formulasi yang mengandungi BMI and 4,4'-diaminodifenilmetana (DDM) pada nisbah 2:1 (BMI/DDM) dengan 0.1 % berat dikumulperoksida (DCP) sebagai pemecut pematangan. Formulasi tersebut menghasilkan komposit dengan masa-gel yang panjang (208 s/g) dan masa pasca-pematangan yang singkat (2 jam) berbanding dengan formulasi lain. Zarah nanosilika (7, 20 dan 130 nm) telah dicampurkan ke dalam matriks BMI/DDM secara kaedah gabungan yang melibatkan pra-rawatan serbuk silika dengan BMI dan adunan-lebur. Silika nanozarah yang tulen didapati berinteraksi dengan matriks polimer melalui ikatan hidrogen manakala zarah silika dengan permukaan yang diubahsuai telah menghasilkan interaksi pengisi-matriks yang kuat melalui ikatan kovalen. Justeru, zarah silika dengan permukaan yang diubahsuai telah menyebabkan peningkatan sifat

mekanik terma SBN seperti E' , T_g dan T_d yang ketara dengan penurunan CTE. Peningkatan sifat-sifat tersebut didapati bergantung kepada kepekatan pengisi, kumpulan berfungsi pada permukaan dan saiz zarah. Secara keseluruhan, sifat mekanik terma yang terbaik bagi SBN telah diperoleh dengan zarah silika bersaiz 7 nm (dicantum dengan kumpulan epoksida) pada kepekatan 10.0 % berat, iaitu E' : 14.1 GPa (pada 30 °C), T_g : 300 °C, α_1 : 28.8 ppm/°C dan $T_{d \text{ (onset)}}$: 451 °C.

SYNTHESIS AND CHARACTERIZATION OF SILICA NANOPARTICLES AND THEIR APPLICATION AS FILLERS IN SILICA-BISMALEIMIDE NANOCOMPOSITE

ABSTRACT

A series of investigations were carried out to study the formation, growth and methods to control the size of silica particles via sol-gel process using tetraethylorthosilicate (TEOS) as the precursor in basic condition. The formation and growth of silica particles were significantly affected by the NH_3 (catalyst) concentration. Lower NH_3 concentrations lead to the formation of stable sols while higher NH_3 concentrations resulted in bigger, spherical silica particles with sizes varying from 90 - 700 nm. In the first approach, the addition of small amount of ammonium salts (NH_4X) produced monodispersed silica particles ranging from 20.5 to 34.1 nm depending on the size and concentration of the anion present in the system. The second approach was conducted to further reduce the silica size by optimizing the reaction parameters such as concentration of TEOS, R (water to TEOS concentration ratio) value, NH_3 feed rate and reaction temperature. The optimal reaction conditions successfully produced highly dispersed ultrafine silica nanoparticles with particle size of 7.1 ± 1.9 nm which falls in the primary size range. The freshly synthesized silica nanoparticles was dispersed and dried using a relatively new, simple and cost effective alcohol-dehydration (AD) technique which was able to suppress the agglomeration and improve the dispersion of silica compared to freeze drying (FD) and oven drying (OD) techniques. The processed silica nanoparticles exhibited some interesting size-dependent properties. Significant increase in the specific surface area (SSA) and silanol concentration (δ_{OH}) and a more gradual increase in the apparent density (D_a) were observed as the particle size was reduced from around 400 to 7 nm. In addition, the decrease in the silanol number (α_{OH})

and Si-O-Si bond angle and the presence of optically active defect sites at smaller particle sizes suggest that the silica structure has been significantly altered at the nanoscale. Chemical modification of silica surface was conducted by grafting epoxide and maleimide groups. The epoxide groups were grafted using 3-glycidyloxypropyltrimethoxysilane (GPTS) while the maleimide groups were grafted by reacting 1,1'-(Methylenedi-4,1-phenylene)bismaleimide (BMI) with silica nanoparticles pre-grafted with amino groups using 3-aminopropyltrimethoxysilane (APTS). Both epoxide and maleimide groups were found covalently bonded to the silica surface and reactive. The loading of functional groups increased with the decrease in the particle size: e.g. 130 nm (1.09 mmol/g) < 20 nm (1.70 mmol/g) < 7 nm (2.04 mmol/g) for the epoxide groups. The matrix for the silica-bismaleimide nanocomposite (SBN) was prepared using a formulation containing BMI and 4,4'-diaminodiphenylmethane (DDM) at 2:1 (BMI/DDM) mol ratio with 0.1 wt.% of dicumylperoxide (DCP) as the curing accelerator. The specified formulation exhibited longer gel-time (208 sec/g) and shorter post-curing time (2 hours) compared to other formulations. The silica nanoparticles (7, 20 and 130 nm) were incorporated into the BMI/DDM matrix using a combination of procedures involving pre-treatments of silica powder in presence of BMI and melt-mixing. The pure silica nanoparticles interacted with the polymer matrix through hydrogen bonding while the surface modified nanoparticles exhibited strong filler-matrix interaction via covalent bonding. Therefore, the surface modified nanoparticles resulted in significant improvements in thermal mechanical properties of SBN such as E' , T_g and T_d and also reduction in CTE. The property enhancements were found dependent on the filler concentration, surface functional group and particle size. Overall, the best thermal mechanical properties were

obtained for SBN containing 7 nm silica particles (grafted with epoxide groups) at 10.0 wt.%, i.e., E' : 14.1 GPa (at 30 °C), T_g : 300 °C, α_1 : 28.8 ppm/°C and T_d (onset): 451 °C.

CHAPTER ONE

INTRODUCTION

1.1 Nanotechnology

On December 29, 1959, Richard Feynman in his famous talk entitled "There's Plenty of Room at the Bottom" has described the possibility of maneuvering things atom by atom in the future [1]. Now, his prediction seems to be realized with the rapid development in nanotechnology. Nanotechnology is rapidly sweeping through all vital fields of science and technology such as electronics and pharmaceuticals with tremendous supports from researchers from both academic and industrial sectors. This is an emerging technology of the 21st century. In the year 2005 alone, US\$ 9.6 billion worth of fund had been dedicated to nanotech research by the governments, corporations and venture capitalists throughout the world [2]. In the same year, US\$ 32 billion worth of goods incorporated with nanotechnology were sold, ranging from General Motors vehicles that includes parts made of polymer-nanoclay composites, to antimicrobial bandages that contains nanosilver particles [2]. Thus, nanotechnology does not only open more room for research and developments but also promises good revenues through commercialization of nanomaterial incorporated products.

The term nanotechnology can be briefly defined as the science and engineering involved in the design, synthesis, characterization, and application of materials and devices on the nanometer scale or one billionth of a meter [3]. In materials where strong bond is present, delocalization of valence electron is extensive and the extent of delocalization depends and varies with the size of the system [4]. This in turn, affects the properties of the material such as chemical properties, magnetic

properties, optical properties, thermal properties and surface reactivity [4]. As a result, nanomaterials often exhibit unique and improved properties compared to the bulk counterparts. Therefore, it provides opportunity to develop new classes of advanced materials which can meet the demands from high-tech industries such as electronics, aerospace, defense and pharmaceutical.

1.2 Nanoceramics

Development of ceramic particles in nano dimension with improved properties has been studied with much success in several areas such as synthesis, surface science and texturology [4]. Ceramic is defined as non-metallic and inorganic, thus all the metal oxides, nitrides and carbides falls in this category [5]. Examples of ceramic are silicon dioxide (silica), aluminum oxide (alumina), titanium dioxide (titania), silicon nitride, and etc. The ceramic materials have been reported to exhibit unique surface chemistry in the nano dimension [6]. Therefore, nanoceramics such as silica nanoparticles have been intensively studied in recent years due to its prospect of application in various commercial fields.

1.2.1 Silica Nanoparticles

Advancement in nanotechnology has lead to the production of nano-sized silica, SiO_2 , which has been widely used in both scientific research and engineering development [7]. Generally, materials with the particle size in the range of 1 – 100 nm are defined as nanomaterials [4, 8-10]. Natural silica is found in plants such as barley, rice husk and bamboo and also in mineral forms of quartz and flint. The silica particles extracted from these natural resources contains metal impurities and not favorable for advanced scientific and industrial applications. Thus, focus is given to synthetic silica

(colloidal silica, silica gels, pyrogenic silica and precipitated silica), which is pure and produced mostly in amorphous powder forms compared to natural mineral silica (quartz, tridymite, cristobalite) which are in crystalline forms [11]. As shown in Figure 1.1, the various methods that have been used to obtain nanomaterials can be categorized into two main approaches: top-down and bottom-up [4, 12]. Top-down is characterized by reducing the dimension of the original size by utilizing special size reduction techniques. Bottom-up approach which involves synthesis of nanomaterials from atomic or molecular scale is the common route used to produce silica nanoparticles. Some of the widely used methods to synthesize silica nanoparticles are sol-gel process, reverse microemulsion and flame synthesis.

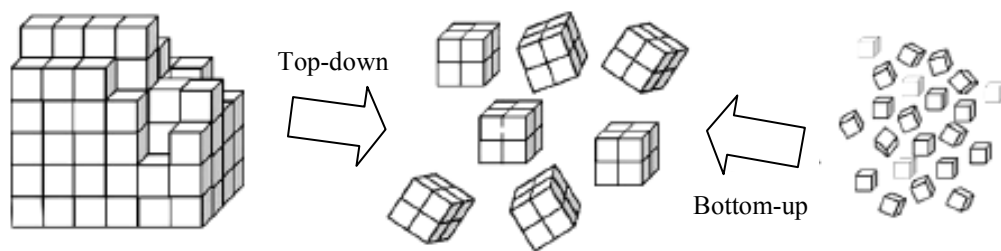


Figure 1.1: Top-down and bottom-up approaches to produce nanomaterials [4, 12].

1.2.1.1 Sol-Gel Process

The sol-gel process is widely applied to produce ceramic materials due to its ability to form pure and homogenous products at mild conditions. The process involves hydrolysis and condensation of metal alkoxides [5, 13] such as tetraethylorthosilicate (TEOS, $\text{Si}(\text{OC}_2\text{H}_5)_4$) or inorganic salts [13] such as sodium silicate (Na_2SiO_3). Silicate particles mostly synthesized in the presence of mineral acid (e.g. HCl) or base (e.g. NH_3) as catalyst. Flow chart of a typical sol-gel process which leads to the production silica nanoparticles using silicon alkoxides ($\text{Si}(\text{OR})_4$), is shown in Figure 1.2.

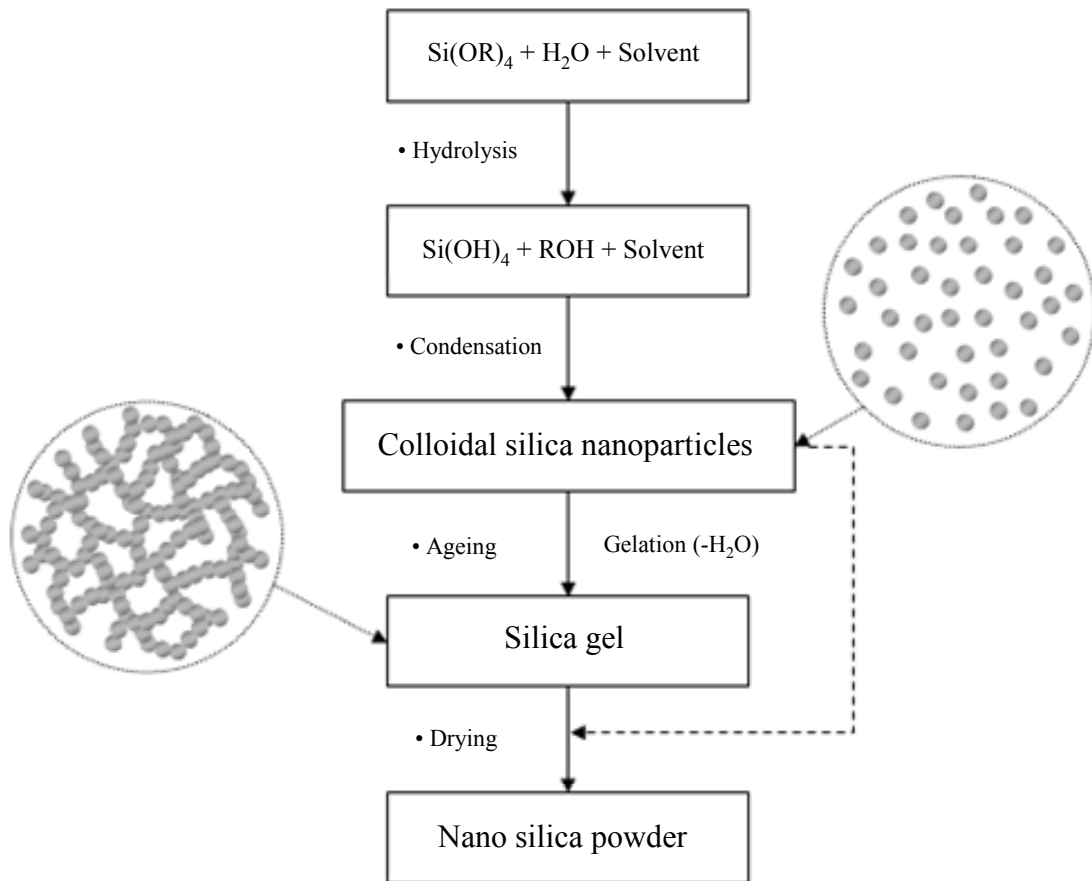


Figure 1.2: Flow chart of a typical sol-gel process for preparing nanosilica powder [6].

Condensation of hydroxide molecules by elimination of water leads to the formation of sol (colloidal silica). After a prolonged ageing process, the colloidal particles will link together to form network structure, resulting in a porous gel. Removal of solvent from the sol or gel will produce silica powder. Since the sol-gel process starts with the nanosized hydroxide units, and undergoes reaction on the nanometer scale, it results in the formation of nanometer silica particles [4]. Optimizing the reaction conditions of sol-gel process such as concentration of reactants, concentration of catalyst and reaction temperature [14, 15] and addition of electrolytes (metal salts) [16] are some of the recent attempts made by the researchers to reduce the silica size using the sol-gel

platform. The smallest possible silica nanoparticles with average diameter of 14 to 20 nm, in colloidal form have been produced using these approaches [14-16].

1.2.1.2 Reverse Microemulsion

Reverse microemulsion (RM) is an efficient method to synthesis monodispersed nanoparticles [17]. In a typical RM system, the surfactants molecules dissolved in organic solvents forms spherical micelles. As illustrated in Figure 1.3, in the presence of water, the polar head groups organize themselves to form microcavities containing water, which is often called as reverse micelles [18]. Synthesis of silica nanoparticles inside the microcavities can be achieved by controlled addition of silicon alkoxides and catalyst into the medium containing reverse micelles. The surfactant stabilized microcavities (in nanometer size) provides a cage-like effect that limits particle nucleation, growth and agglomeration [19, 20], leading to the formation of homogenous silica nanoparticles. Major drawbacks of the RM approach are the high cost and difficulties in the removal of surfactants after the synthesis [21].

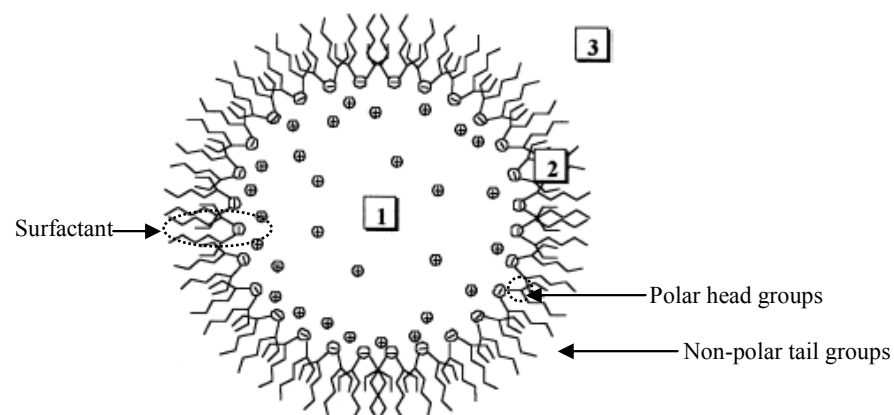


Figure 1.3: Schematic representation of reverse micelles, showing the different regions of a micellar solution: (1) water pool; (2) interface; and (3) organic phase [18].

1.2.1.3 Flame Synthesis

Silica nanoparticles also can be produced through high temperature flame decomposition of metal-organic precursors. This process also referred as chemical vapor condensation (CVC) [3]. In a typical CVC process, silica nanoparticles are produced by burning silicon tetrachloride, SiCl_4 with hydrogen and oxygen [11]. Difficulty in controlling the particle size, morphology and phase composition is the main disadvantages of the flame synthesis [4]. Nevertheless, this is the prominent method that has been used to commercially produce silica nanoparticles in powder form.

1.2.2 Applications of Silica Nanoparticles

Silica nanoparticles are widely used in high-tech applications owing to their many attractive properties such as excellent physical, chemical, mechanical and sintering properties [4]. At present, silica nanoparticles are extensively studied for their prospective as photonic crystals [22, 23], chemical sensors [24], biosensors [25], nanofillers for advanced composite materials [26-28], markers for bioimaging [29], substrate for quantum dots [30, 31] and catalysts [32, 33], and etc. Optical absorption and emission properties, concentration of silanol groups, specific surface area and density are some of the key parameters that govern the utilization of silica nanoparticles in the contemporary research works. However, literatures describing the size-dependent properties and contemporary application of silica nanoparticles are still lacking at the moment.

1.2.3 Agglomeration and Aggregation Problems in Silica Nanoparticles

The extents of agglomeration and aggregation in silica nanoparticles are important parameters that govern their utility in various types of application. Agglomeration is the sharing of a plane or side between two particles, while aggregation indicates one-point linking of particles [11]. The presence of agglomerates and aggregates will readily affect the physical properties such as surface area. Therefore, agglomeration and aggregation-free nanoparticles are essential in ceramics, composites and electronics applications [34]. It has been reported that the agglomeration can be reduced by appropriate drying of the sol or gel that carries the nanoparticles [35]. On the other hand, chemical modification of silica surface has been proven to effectively reduce the aggregation phenomena [11].

1.3 Silica-Polymer Nanocomposites

In principle, the incorporation of inorganic moieties (fillers) with organic polymeric materials (matrix) results in the formation of composite materials [8]. Once, one of the dimensions of the filler material is of the order of a nanometer scale or more definitively in the range of 1 - 100 nm, it is termed as nanocomposite [4, 8-10]. The final product does not have to be in nanoscale, but can be micro- or macroscopic in size [36]. The resulting inorganic-organic hybrid materials, which is also often called as the polymer matrix composite (PMC), have been proven to exhibit excellent properties in terms of thermal, mechanical, electrical and magnetic behaviors compared to the pure organic polymer due to the synergism between the properties of the components [8]. Exceptionally low coefficient of thermal expansion (CTE) of silica caused by the high Si-O bond energy has made the silica filled PMCs widely studied, especially for the applications at elevated temperatures such as in semiconductor packaging [7].

The application of silica nanoparticles as fillers in the preparation of advance PMC has drawn much attention in recent years. This is due to the increased demand for new materials with improved thermal, mechanical, physical and chemical properties, especially for the application in semiconductor packaging, aerospace and defense related industries. Recent developments in the synthesis of monodispersed, narrow size distributed silica nanoparticles are realized to provide significant boost to the development of silica-polymer nanocomposites. Silica nanoparticles which exhibit significantly higher specific surface area and silanol concentration compared to the bulk silica [4] is expected to drastically alter the properties of polymer composite with respect to macroscopic composites that are made of the same components. In the case of particle filled composite system, the surface area per unit volume is inversely proportional to the material's diameter. Thus, greater surface area per unit volume (A/V ratio) is achieved with smaller particle size [37, 38]. Higher A/V ratio results in increased interaction between the nanoparticles and polymer matrix, leading to various property enhancements.

Generally, three types of nanocomposite can be prepared by varying the type of chemical interaction between the inorganic-organic components in PMC, i.e., (i) strongly bonded (via covalent, coordination, ionic interactions); (ii) weakly bonded (van der Waals, hydrogen-bonding interactions); and (iii) without chemical interactions [39, 40]. A critical challenge in the design of these hybrid inorganic-organic systems is the ability to control the mixing between the two dissimilar components or phases [8]. Homogenous mixing of the inorganic-organic components can be achieved by surface modification of silica nanoparticles.

1.3.1 Surface Modification of Silica Nanoparticles

Physical mixtures of organic polymers and preformed silica nanoparticles may lead to phase separation, resulting in poor mechanical, thermal, optical and etc. properties [8]. The hydrophilic nature of silica surface shows restricted affinity towards the polymer matrix [7]. In addition, silica nanoparticles tend to form aggregates during the formation of nanocomposite due to the inter-particle interactions. According to Kickelbick [8], there are five possibilities to overcome the phase separation in hybrid particulate systems, i.e., (i) the use of a polymer which weakly interacts (secondary bondings) with the nanoparticles; (ii) the covalent attachment of an inert organic layer on the surface of the particle to serve as a compatibilizer at the particle/polymer interface; (iii) the encapsulation of the particles through emulsion polymerization; (iv) the attachment of functional groups which allow a covalent linkage with the polymer; and (v) the attachment of initiation groups for grafting of polymer chains from the particle surface. Among the five different methods, attachment of functional groups which could form covalent bonding with the polymer matrix is relatively popular and used by many researchers to impart strong interfacial bonding in the nanocomposite.

In the case of silica based nanocomposites, silane coupling agents, $\text{Si}(\text{OR})_3\text{R}'$ are widely used to functionalize the hydrophilic silica surface [41-43], where the functional groups, R' , introduced to the silica surface via condensation of silanol groups ($\equiv\text{Si-OH}$) with the alkoxy groups, $-\text{OR}$. The selection of desirable functional group (R') depends on the subject of application.

1.3.2 Selection of Polymer Matrix

In order to exploit the full potential of the technological applications of the nanomaterials, it is very important to endow them with good processability which has ultimately guided scientists to use conventional polymers as one component of the nanocomposites [44]. The conventional polymer matrixes used in the preparation of composite materials can be classified into two main categories: thermoplastics and thermosets. A thermoplastic is a plastic that melts to a liquid when heated and freezes to a glassy state when cooled sufficiently. Thermoplastics often have only very weak intermolecular forces between non-oriented chain segments [45]. Examples of thermoplastics are acrylic, acetate, nylon, polyethylene, polystyrene and etc. On the other hand, thermosetting plastics or thermosets are polymer materials that irreversibly cure, to a stronger form [46]. Upon curing, the thermoset will form permanent network structures through formation intermolecular cross-links (covalent bonds) between the polymer chains [45, 46]. Thus, it exhibits good dimensional stability and resist viscous flow at elevated temperature compared to the thermoplastics. Therefore, thermosets are often used as the matrix for the preparation of advanced composite materials that can meet common engineering needs of high temperature applications such as in aerospace, defense and semiconductor packaging industries. Epoxies, poly(arylene ethers), polyurethanes, polybenzimidazoles, bismaleimides, organofluoro polymers, certain silicones and liquid crystalline polyesters are some of the common commercially available thermosets.

1.3.2.1 Epoxies

At present, epoxy resins such as diglycidyl ether of Bisphenol A (DGEBA) are widely used as the matrix for the preparation of silica-polymer nanocomposite. The main advantages of epoxies are they are easy to handle and show good processability. However, the silica-epoxy nanocomposites are not favorable for applications above 250 °C due to their low T_g , i.e., 165 – 240 °C [47, 48]. In addition, the incorporation of silica nanoparticles has been reported to decrease the T_g of the neat epoxy polymer by 7 to 12 °C with the increase in the filler loading from 15 to 50 wt.% [47, 48]. Thus, it is necessary to find new classes of silica-thermoset nanocomposites which can withstand high temperature with minimal loss in the thermal mechanical properties as compared to the conventional epoxies. Thermosetting polyimide resins such as bismaleimides and nadimides are being favorably considered as replacements for epoxy resins in certain commercial and military applications [49].

1.3.2.2 Bismaleimide

The bismaleimide (BMI) systems dominate over the other thermosetting polymer matrices primarily due to their high performance-to-cost ratio and relatively high temperature resistance (e.g. high T_g and T_d and low CTE) [50]. Besides, BMI also offers superior thermal and oxidative stability, low susceptibility for moisture absorption and good flame retardance. The main advantage of BMI is that it can withstand high stress at high temperatures at which typical epoxies, phenolics and most of the high performance plastics are unstable [51]. One disadvantage of BMI is that it is relatively brittle due to their aromatic nature and high cross-linking density. Therefore, many BMI resins have been modified through various chain extension reactions to enhance their fracture toughness. Co-polymerizing the maleimide double bond with

aromatic diamine such as 4, 4'-diaminodiphenylmethane (DDM) is one of the most efficient and cost-effective method to achieve this objective [52-54]. Some of the reported inorganic-BMI composites are carbon-BMI [55-57], clay-BMI [58] and potassium titanate-BMI [59] hybrids. However, works on silica nanoparticles-BMI composites have not been reported in the literatures, thus the opportunity to develop such material is still open.

1.4 Problem Statements

The research developments addressed in the above sections would have given some brief pictures on the synthesis and applications of silica nanoparticles. Following are some of the challenges and opportunities that exist in the contemporary research in silica nanoparticles:

- (a) At present, the synthesis of monodispersed and narrow size distributed silica nanoparticles significantly below 10 nm, in powder form via sol-gel process is not much reported in the literatures. Most of the reported works focused on the synthesis of colloidal silica nanoparticles. Preparation of silica nanoparticles in powder form would benefit many applications which require solvent free nanoparticle systems that are easy to handle and store;
- (b) To date, methods to control the agglomeration of the sol-gel derived silica nanoparticles is not much reported in the literatures. Effective drying techniques could reduce the agglomeration of silica nanoparticles;
- (c) Literatures on size-dependent properties of silica nanoparticles are still lacking due to difficulty in producing silica nanoparticles in well defined size ranges and from the same origin.

- (d) As described earlier, the incorporation of silica nanoparticles into BMI polymer matrix would yield potentially a new class of nanocomposite, which is not much reported. Chemical modification of silica surface with BMI compatible organo-functional groups and preparation of BMI polymer matrix are two important steps that have to be passed prior to the preparation of silica-BMI nanocomposite.

1.5 Research Objectives

The main objectives of this study are;

- (a) To establish effective method(s) to synthesize monodispersed and narrow size distributed silica nanoparticles especially below 10 nm by;
 - (i) Studying the effect of electrolytes (ammonium salts) on the formation of silica nanoparticles in the sol-gel process, and;
 - (ii) Investigating the important experimental parameters that govern the growth and size of the silica particles in the sol-gel process.
- (b) To study the effect of drying technique(s) on the morphology of silica nanoparticles;
- (c) To determine the size-dependent properties of silica nanoparticles;
- (d) To conduct chemical modification of silica surface by grafting organo-functional group(s);
- (e) To develop a bismaleimide-diamine polymer matrix with optimal formulation and curing conditions, and;
- (f) To explore the potential of silica nanoparticles prepared in this study as fillers in silica-bismaleimide nanocomposite system.

1.6 Scope of the Study

This study emphasizes on the synthesis, characterization and chemical modification of ultrafine silica nanoparticles and evaluates its potential application as fillers in a potentially novel PMC, i.e., silica-bismaleimide nanocomposite. The works conducted in this research can be categorized into three parts, i.e., (i) inorganic, (ii) organic, and (iii) inorganic-organic hybrid. The inorganic part involves the synthesis, characterization and surface modification of silica nanoparticles while the organic part includes the preparation of BMI/DDM polymer matrix. On the other hand, the hybrid part entails the preparation and characterization of silica-bismaleimide nanocomposites.

In the first part, two approaches are used to produce smallest possible silica nanoparticles via sol-gel process, i.e., via (i) addition of electrolytes (ammonium salts) and (ii) optimization of reaction parameters (reagents and conditions). The efficiency of the synthesis routes are evaluated based on the resulting particle size, morphology and yield. This followed by an investigation on drying techniques, aimed to reduce the agglomeration of silica nanoparticles in powder form. Focus is given to develop a new and cost effective drying technique based on alcohol dehydration to remove the liquid phase from the suspension that contains the silica nanoparticles. Next, the size dependent properties of silica nanoparticles are studied using various solid state characterization techniques. The study centers on the determination of some important physical, chemical and optical properties of silica nanoparticles. Subsequently, chemical modifications of silica surface are conducted to graft some selected organo-functional groups, i.e., epoxide and maleimide groups onto the silica surface. Characterization of the modified silica surfaces and determination of the functional

groups' reactivity are the main emphasis of this fraction of study. The second part focused on the preparation of BMI/DDM polymer matrix with optimal formulation and curing conditions. Finally, the third part involves the preparation and characterization of silica-bismaleimide nanocomposites. In this part, the effects of filler concentration, surface functional groups and particle size on the resulting thermal mechanical properties of silica-bismaleimide nanocomposites are studied. In addition, the effect of fillers on the curing profile of BMI/DDM polymer matrix and chemical interaction between the fillers and polymer matrix are also investigated.

1.7 Thesis layout

This thesis is composed of 11 chapters. Chapter 1 provides a brief introduction to highlight current state of research on silica nanoparticles and the objectives of the study. Chapter 2 consists of literature studies, mainly on the synthesis of silica nanoparticles via sol-gel process, agglomeration of silica nanoparticles, the size-dependent properties, silica-polymer nanocomposites, chemical modification of silica surface and bismaleimide polymer matrix. The experimental procedures which are compilation of experimental methods for Chapter 4 to 10 are described in Chapter 3. Chapters 4 to 10 are actually results and discussion chapters which serve the research objectives listed in Section 1.5, in a similar order. Chapter 4 and 5 describes the synthesis of silica nanoparticles in the presence of electrolytes and under optimized reaction conditions of sol-gel process, respectively. Chapter 6 elaborates the effects of drying techniques on the morphology of silica nanoparticles while Chapter 7 reports the size-dependent properties of silica nanoparticles. Chapter 8 conveys the chemical modification of silica surface using various organo-functional groups. The preparation and characterization of BMI/DDM polymer matrix and silica-bismaleimide

nanocomposite are discussed in Chapter 9 and 10, respectively. Finally, the thesis ends with conclusion and recommendation for future research in Chapter 11.

References

1. Drexler, K. E. (1986). *Engines of Creation: The coming era of nanotechnology*. Doubleday/Anchor Press, New York.
2. Nordan, M. M. (2006). Nanotechnology's impact today - and how to make sense of it (Business Spotlight). *Advanced Materials and Processes*. **August Issue**: 37.
3. Silva, G. A. (2004). Introduction to nanotechnology and its applications to medicine. *Surgical Neurology* **61**: 216.
4. Klabunde, K. J. (2001). *Nanoscale materials in chemistry*. Wiley-Interscience, New York.
5. Brinker, C. J. and Scherer, G. W. (1990) *Sol-Gel Science: The physics and chemistry of sol-gel processing*. Academic Press Inc., San Diego.
6. Klabunde, K. J., Stark, J. V., Koper, O., Mohs, C., Park, D. G., Decker, S., Jiang, Y., Lagadic, I., and Zhang, D. (1996). Nanocrystals as stoichiometric reagents with unique surface chemistry. *J. Phys. Chem.* **100**: 12142.
7. Sun, Y., Zhang, Z. and Wong, C. P. (2005). Study on mono-dispersed nano-size silica by surface modification for underfill applications. *J. Colloid Inter. Sci.* **292**: 436.
8. Kickelbick, G. (2003). Concepts for the incorporation of inorganic building blocks into organic polymers on a nanoscale. *Prog. Polym. Sci.* **28**: 83.
9. Zeng, Q. H., Wang, D. Z. Yu, A. B. and Lu, G. Q. (2003). Synthesis of polymer-montmorillonite nanocomposites by in situ intercalative polymerization. *Nanotechnology* **13**: 549.
10. Wang, Z. and Pinnavaia, J. T. (1998). Nanolayer reinforcement of elastomeric polyurethane. *Chem. Mater.* **10**: 1820.
11. Vansant, E. F., Voort, P. V. D. and Vrancken, K. C. (1995). *Characterization and chemical modification of the silica surface*, Elsevier Science, New York.
12. Reverchon, E. and Adami, R. (2006). Nanomaterials and supercritical fluids. *J. Supercritical Fluids* **37**: 1.
13. Iller, R. K. (1979). *The chemistry of silica and silicates*, Wiley, New York.
14. Park, S. K., Kim, K. D. and Kim, H. T. (2002). Preparation of silica nanoparticles: determination of the optimal synthesis conditions for small and uniform particles, *Colloids Surf. A.* **197**: 7.

15. Rao, K. S., Hami, K. E., Kodaki, T., Matsushige, K. and Makino, K. (2005). A novel method for synthesis of silica nanoparticles. *J. Colloid Inter. Sci.* **289**: 125.
16. Kim, S. S., Kim, H. S., Kim, S. G. and Kim, W. S. (2004). Effect of electrolyte additives on sol-precipitated nano silica particles. *Ceramics Inter.* **30**: 171.
17. Petit, C., Lixon, P. and Pileni, M. P. (1990). Synthesis of cadmium sulfide in situ in reverse micelles. 2. Influence of the interface on the growth of the particles. *J. Phys. Chem.* **94**: 1598.
18. Silber, J. J., Biasutti, A., Abuin, E. and Lissi, E. (1999). Interactions of small molecules with reverse micelles. *Adv. Colloid Inter. Sci.* **82**: 189.
19. Leung, R., Hou, M. J. and Shah, D. O. in: Wasan, D. T., Ginn, M. E. and Shah D. O. (Eds.) (1988), *Surfactant Science Series, vol. 28*, Marcel Dekker, New York.
20. Pillai, V. and Shah, D. O. in: Soalns, C and Kunieda H. (Eds.) (1997) *Industrial Application of Microemulsion*, Marcel Dekker, New York.
21. Buining, P. A., Liz-Marza'n, L. M., and Philipsea, A. P. (1996). Simple preparation of small, smooth silica spheres in a seed alcosol for Stöber synthesis. *J. Colloid Interface Sci.* **179**: 318.
22. Chiappini, A., Armellini, C., Chiasera, A., Ferrari, M., Jestin, Y., Mattarelli, M., Montagna, M., Moser, E., Conti, G. N., Pelli, S., Righini, G. C., Gonçalves, M. C. and Almeida, R. M. (2007). Design of photonic structures by sol-gel-derived silica nanospheres. *J. Non-Cryst. Solids* **353**: 674.
23. Pallavidino, L., Razo, D. S., Geobaldo, F., Balestreri, A., Bajoni, D., Galli, M., Andreani, L. C., Ricciardi, C., Celasco, E., Quaglio, M. and Giorgis, F. (2006). Synthesis, characterization and modeling of silicon based opals. *J. Non-Cryst. Solids* **352**: 1425.
24. Wang, C. T., Wu, C. L., Chen, I. C. and Huang, Y. H. (2005). Humidity sensors based on silica nanoparticle aerogel thin films. *Sens. Actuators B.* **107**: 402.
25. Grant, S. A., Weilbaecher, C. and Lichlyter, D. (2007). Development of a protease biosensor utilizing silica nanobeads. *Sens. Actuators B.* **121**: 482.
26. Wang, H., Bai, Y., Liu, S., Wu, J. and Wong, C. P. (2002). Combined effects of silica filler and its interface in epoxy resin. *Acta Mater.* **50**: 4369.
27. Zhang, H., Zhang, Z., Friedrich, K. and Eger, C. (2006). Property improvements of in situ epoxy nanocomposites with reduced interparticle distance at high nanosilica content. *Acta Mater.* **54**: 1833.

28. Kwon, S. C., Adachi, T., Araki, W. and Yamaji, A. (2006). Thermo-viscoelastic properties of silica particulate-reinforced epoxy composites: Considered in terms of the particle packing model. *Acta Mater.* **54**: 3369.
29. Sharma P., Brown S., Walter G., Santra, S. and Moudgil, B. (2006). Nanoparticles for bioimaging. *Adv. Colloid Interface Sci.* **123**: 471.
30. Jiang, L., Wang, W., Wu, D., Zhan, J., Wang, Q., Wu, Z. and Jin, R. (2007) Preparation of silver quantum dots embedded water-soluble silica/PAAc hybrid nanoparticles and their bactericidal activity. *Mater. Chem. Phys.* **104**: 230.
31. Lai, C. Y., Wu, C. W., Radu, D. R., Trewyn, B. G. and Lin, V. S. Y. (2007). Reversible binding and fluorescence energy transfer between surface-derivatized CdS nanoparticles and multi-functionalized fluorescent mesoporous silica nanospheres. *Stud. Surf. Sci. Catal.* **170**: 1827.
32. Neri, G., Rizzo, G., Crisafulli, C., Luca, L. D., Donato, A., Musolino, M. G. and Pietropaolo, R. (2005). Isomerization of α -pinene oxide to campholenic aldehyde over Lewis acids supported on silica and titania nanoparticles. *Appl. Catal. A* **295**: 116.
33. Gole, J. L., Burda, C., Wang, Z. L. and White, M. (2005). Unusual properties and reactivity at the nanoscale. *J. Phys. Chem. Solids* **66**: 546.
34. Pratsinis, S.E. (1998). Flame aerosol synthesis of ceramic powders. *Prog. Energy Combust. Sci.* **24**: 197.
35. Kwon, S. and Messing, G. L. (1997). The effect of particle solubility on the strength of nanocrystalline agglomerates: Boehmite, *NanoStruc. Mater.* **8**: 399.
36. Hussain, F., Hojjati, M., Okamoto, M. and Gorga, R. E. (2006). Polymer-matrix nanocomposites, processing, manufacturing, and application: An overview. *J. Composite Materials* **40**: 1511.
37. Luo, J. J. and Daniel, I. M. (2003). Characterization and modeling of mechanical behavior of polymer/clay nanocomposites. *J. Compos. Sci. Technol.* **63**:1607.
38. Thostenson, E., Li, C. and Chou, T. (2005). Review nanocomposites in context. *J. Compos. Sci. Technol.* **65**: 491.
39. Judeinstein, P. and Sanchez, C. (1996). Hybrid organic–inorganic materials: a land of multidisciplinary. *J. Mater. Chem.* **6**: 511.
40. Schubert, U. and Husing, N. (2000). *Synthesis of inorganic materials*. Wiley–VCH, Weinheim.

41. Jesionowski, T. and Krysztafkiewicz, A. (2002). Preparation of the hydrophilic/hydrophobic silica particles. *Colloids Surfaces A*. **207**: 49.
42. Fonseca, M. G., Oliveira, A. S. and Airoidi, C. (2001). Silylating agents grafted onto silica derived from leached chrysotile. *J. Colloid Interface Sci.* **240**: 533.
43. Yu, Y. Y., Chen, C. Y. and Chen, W. C. (2003). Synthesis and characterization of organic–inorganic hybrid thin films from poly(acrylic) and monodispersed colloidal silica. *Polymer* **44**: 593.
44. Gangopadhyay, A. and De, A. (2000). Conducting polymer nanocomposites: A brief overview. *Chem. Mater.* **12**: 608.
45. Elias, H. G. (1996). *An introduction to polymer science*. VCH Publishers, New York.
46. Pascault, J. P., Sautereau, H., Verdu, J. and Williams, R. J. J. (2002). *Thermosetting polymer*. Marcel Dekker, Inc. New York.
47. Ragosta, G., Abbate, M., Musto, P., Scarinzi, G. and Mascia, L. (2005). Epoxy-silica particulate nanocomposites: Chemical interactions, reinforcement and fracture toughness. *Polymer* **46**: 10506.
48. Liu, Y. L., Hsu, C.Y., Wei, W. L. and Jeng, R. J. (2003). Preparation and thermal properties of epoxy-silica nanocomposites from nanoscale colloidal silica. *Polymer* **44**: 5159.
49. Torrecillas, R., Regnier, N and Mortaigne, B. (1996). Thermal degradation of bismaleimide and bisnadimide networks-products of thermal degradation and type of crosslinking points. *Polym. Degrade. Stab.* **51**: 307.
50. Lin S. C. and Pearce, E M. (1993). *High performance thermoset: Chemistry, properties and applications*, Hanser, Munich.
51. Kumar, K. S. S., Nair, C. P. R., Sadhana, R. and Ninan K. N. (2007). Benzoxazine–bismaleimide blends: Curing and thermal properties. *Euro. Polym. J.* **43**: 5084.
52. Guilio, C. D., Gautier, M. and Jasse, B. (1984). Fourier transform infrared spectroscopic characterization of aromatic bismaleimide resin cure states. *J. App. Polym. Sci.* **29**: 1771.
53. Loustalot, M. F. G. and Cunha, L. D. (1997). Study of molten-state polymerization of bismaleimide monomers by solid-state ¹³C n.m.r. and FTi.r. *Polymer* **39**: 1833.
54. Wu, W., Wnag, D. and Ye, C. (1998). Preparation and characterization of bismaleimide-diamine prepolymers and their thermal-curing behavior. *J. App. Polym. Sci.* **70**: 2471.

55. Bao, L. R. and Yee, A. F. (2002). Effect of temperature on moisture absorption in a bismaleimide resin and its carbon fiber composites. *Polymer* **43**: 3987.
56. Bao, L. R. and Yee, A. F. (2002). Moisture diffusion and hygrothermal aging in bismaleimide matrix carbon fiber composites: part II—woven and hybrid composites. *Compos. Sci. Technol.* **62**: 2111.
57. Parka, J. M., Kim, J. W. and Yoon, D. J. (2002). Interfacial evaluation and microfailure mechanisms of single carbon fiber/bismaleimide (BMI) composites by tensile and compressive fragmentation tests and acoustic emission. *Compos. Sci. Technol.* **62**: 743.
58. Meng, J. and Hu, X. (2004). Synthesis and exfoliation of bismaleimide–organoclay nanocomposites. *Polymer* **45**: 9011.
59. Liang, G., Hu, X. and Lu, T. (2005). Inorganic whiskers reinforced bismaleimide composites (Part II). *J. Mater. Sci.* **40**: 1743.

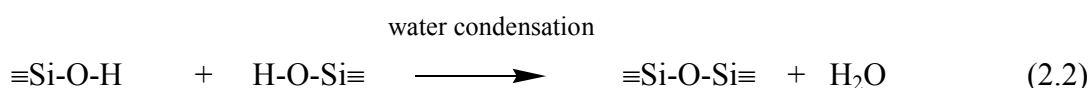
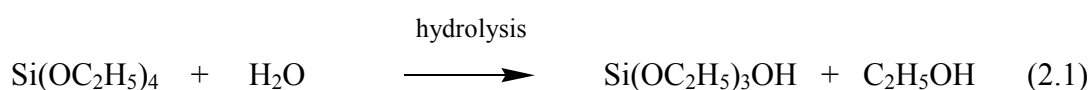
CHAPTER TWO

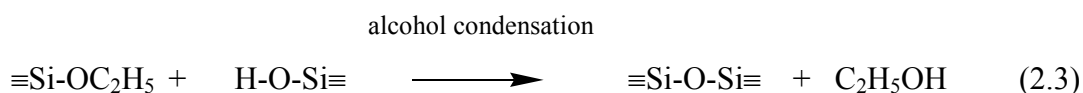
LITERATURE REVIEWS

2.1 Sol-Gel Process

Interest in sol-gel processing of inorganic ceramics materials began in the mid-1800s with the initial works reported by Ebelmen [1] and Graham [2] on silica gels. Their works dealt with hydrolysis of tetraethylorthosilicate (TEOS), $\text{Si}(\text{OC}_2\text{H}_5)_4$, under acidic conditions which eventually produced ‘glass like’ silica materials. In the period of 1950 to 1960, Roy and co-workers used the sol-gel method to produce various types of novel ceramics containing Al, Si, Zr, Ti, etc. [3-5]. In the same period, Iller’s prominent works in silica chemistry [6] made significant impact on further development of sol-gel process. Iller’s contributions led to the first commercial production of colloidal silica nanoparticles called Ludox[®], by Du Pont Chemicals Company [7].

The sol-gel process is widely used to produce homogenous and pure silica particles under mild conditions. It provides many advantages such as the ability to control the particle size, size distribution and morphology of silica compared to other techniques like flame synthesis and microemulsion route. The general reactions of TEOS that leads to the formation of silica particles in the sol-gel process can be written as [7-10]:





The hydrolysis of TEOS molecules forms silanol groups. The polycondensation between the silanol groups or between silanol groups and ethoxy groups creates siloxane bridges (Si-O-Si) that forms the entire silica structure [10]. The polycondensation reaction also often referred as polymerization [6]. The polymerization rate depends on reaction conditions which might result in the formation of either a three dimensional network or single monodispersed particles [11]. According to Iller [6], the polymerization occurs in three stages i.e., (i) polymerization of monomers to form primary particles, (ii) growth of the particles, and (iii) linking of particles into chains and then networks which forms the gel structure. In addition, he also stated that the condensation reactions takes place in such a fashion as to maximize the number of Si-O-Si bonds and minimize the terminal hydroxyl (silanol) groups through internal condensation [6]. In general, the formation of silica particles can be divided into two stages: nucleation and growth. Figure 2.1 shows the polymerization behavior of aqueous silica, given by Iller [6]. As shown in the figure, in basic condition (B), the particles grow in size and decrease in number through Oswald ripening mechanism [10]. By contrast, in acidic condition (A) or in presence of flocculating salts the particles aggregates into three-dimensional networks and form gels.

Two models, monomer addition [12, 13] and controlled aggregation [9, 14] have been proposed to describe the growth mechanism of silica. The monomer addition model describes that after an initial burst of nucleation the particle growth occurs through the addition of hydrolyzed monomers onto the (primary) particle surface. By

contrast, the aggregation model elaborates that the nucleation occurs continuously throughout the reaction and the resulting nuclei (primary particles) will aggregate together to form larger particles (secondary particles).

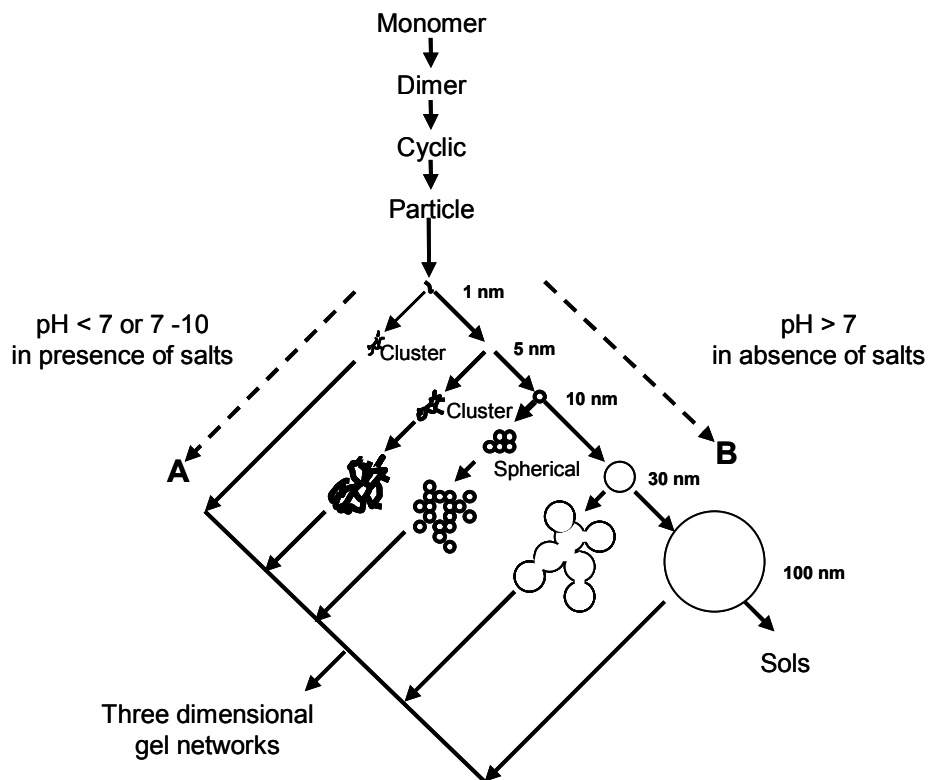


Figure 2.1: Polymerization behavior of aqueous silica [6].

According to Brinker and Scherer [10], in basic conditions the particle growth occur predominantly by monomer addition or monomer-cluster aggregation (MCA) kinetic model. This model is further divided into diffusion limited monomer-cluster aggregation (DLMCA) and reaction limited monomer-cluster aggregation (RLMCA) mechanisms. According to DLCMA, monomers ($\text{Si}(\text{OH})_4$) travel by random walks and stick irreversibly (condensation reaction) at first contact with the growing cluster. Opposite to the DLMCA, RLMCA provides that condensation between monomer and